

# SHEAR STRENGTH OF CONCRETE-ENCASED COMPOSITE STRUCTURAL MEMBERS

By C. C. Weng,<sup>1</sup> S. I. Yen,<sup>2</sup> and C. C. Chen<sup>3</sup>

**ABSTRACT:** This study investigates the shear strength of composite steel and concrete members in which the steel shape is fully encased in concrete. Two types of shear failure—diagonal shear and shear bond—are examined in this study. Through understanding of these failure modes, a new approach is proposed to predict the shear capacities of composite members. Major parameters investigated include steel flange width, shear reinforcement, concrete strength, and applied axial load. To evaluate the accuracy of the proposed approach, a verification analysis is made by comparing shear capacities predicted by the proposed approach with previous test results. Furthermore, the shear capacities predicted by the proposed approach are also compared with those obtained by American and Japanese provisions. The results of the analysis and comparison indicate that the proposed approach yields satisfactory prediction of shear strength and provides a rational explanation on the mechanism of shear bond failure. A new term, the critical steel flange ratio, is introduced to distinguish the shear bond failure from the conventional diagonal shear failure.

## INTRODUCTION

The composite steel and reinforced concrete structural system can form a building carrying the merits of each material. Preventing shear failure is one of the major concerns when designing a composite structural member. The shear failure of a concrete-encased composite member generally involves two possible failure modes: (1) the diagonal shear failure, which closely resembles the shear failure of an ordinary reinforced concrete structural member; and (2) the shear bond failure (as shown in Fig. 1), which results in cracks along the interface of the steel flange and concrete. For a composite member, the shear bond failure can be critical when the steel flange width is large and approaching the overall width of the composite section. Experiments conducted in Japan have shown that shear bond cracks along the interface of the steel flange and concrete are responsible for early failure of some tested concrete-encased composite members (Wakabayashi 1988; Zhang 1993).

Among the shear design approaches developed for concrete-encased composite members, the design provisions suggested by the American building specifications and by the Japanese building codes are two widely employed approaches. In the United States, the design provisions of composite members can be found in the American Concrete Institute (ACI) (1999) building code, the American Institute of Steel Construction (AISC) (1993) LRFD specification, and the NEHRP seismic provisions [Building Seismic Safety Council (BSSC) (1997)]. In the ACI code, the concrete and the transverse reinforcement provide the shear resistance of the concrete-encased composite member. However, no design provision is available to prevent the possible shear bond failure. In the AISC-LRFD specification (Chapter I), the steel web is responsible for the shear resistance of the composite member; but the contribution of the concrete and transverse reinforcement is conservatively neglected. In the NEHRP provisions (Chapter 7), although the steel web and the transverse reinforcement are taken into ac-

count for the shear resistance of the composite member, the concrete part is not included. Most importantly, both of the AISC and NEHRP provisions do not provide design guidance to avoid the shear bond failure that may occur along the interface of the steel flange and concrete of a concrete-encased composite member.

In Japan, the concept of superposition for the shear design of composite members is adopted in the Architectural Institute of Japan (AIJ) steel reinforced concrete (SRC) building code (AIJ 1987). The shear bond failure mode is considered in the design code. Although the Japanese guidelines are comprehensive for design of composite members, much of the guidelines are not applicable to U.S. construction due to differences in design practice (Ricles 1994).

It is noted that a 5-year research program on composite and hybrid structures (Goel 1997; Nishiyama 1998) as phase 5 of the U.S.-Japan cooperative earthquake research program was initiated in 1993. This program was organized into the following four groups: (1) concrete-filled tube column systems; (2) reinforced concrete and steel reinforced concrete column systems; (3) hybrid wall systems; and (4) research for innovation on new materials, elements, and systems. The program objectives are to develop practical analysis and design procedures for structures in the first three groups and feasibility studies of new and innovative structural elements and composite systems in the fourth group. However, as for the study on the shear strength of concrete-encased composite members, further research is needed on the behavior of the shear bond failure mechanism.

In light of the above discussion, this study presents a new approach to predict the shear strengths of concrete-encased composite members. The proposed approach considers the possible failure modes of diagonal shear failure and shear bond failure. In addition, the approach proposed herein attempts to

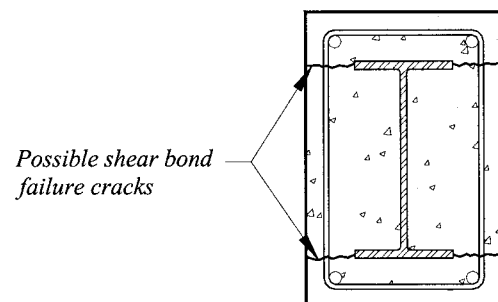


FIG. 1. Shear Bond Failure Cracks along Interfaces of Steel Flanges and Concrete

<sup>1</sup>Prof., Dept. of Civ. Engrg., Nat. Chiao Tung Univ., 1001 Ta Hsueh Rd., Hsinchu, 30050, Taiwan. E-mail: weng@cc.nctu.edu.tw

<sup>2</sup>Grad. Res. Asst., Dept. of Civ. Engrg., Nat. Chiao Tung Univ., 1001 Ta Hsueh Rd., Hsinchu, 30050, Taiwan.

<sup>3</sup>Assoc. Prof., Dept. of Civ. Engrg., Nat. Chiao Tung Univ., 1001 Ta Hsueh Rd., Hsinchu, 30050, Taiwan.

Note. Associate Editor: Amir Mirmiran. Discussion open until March 1, 2002. To extend the closing date one month, a written request must be filed with the ASCE Manager of Journals. The manuscript for this paper was submitted for review and possible publication on June 26, 1998; revised April 2, 2001. This paper is part of the *Journal of Structural Engineering*, Vol. 127, No. 10, October, 2001. ©ASCE, ISSN 0733-9445/01/0010-1190-1197/\$8.00 + \$.50 per page. Paper No. 18653.

correspond to the format of the ACI and AISC approaches. To evaluate the accuracy of the proposed approach, a verification analysis between shear capacities computed by the proposed approach and experimental results done by other researchers is made.

Also performed herein is a series of parametric studies to investigate the major parameters that may affect the failure mode of a composite member. These parameters include the steel flange width, stirrup ratio, concrete strength, and applied axial load. A new factor called "the critical steel flange ratio" is introduced to distinguish the failure modes between diagonal shear failure and shear bond failure of a composite member. Finally, the shear capacities predicted by using the proposed approach, the AIJ-SRC code, the ACI code, the AISC-LRFD specification, and the NEHRP provisions are compared. The related shear design provisions of these codes and specifications are briefly reviewed in the following sections.

### AIJ-SRC CODE (AIJ 1987)

According to the AIJ-SRC code (AIJ 1987), the shear capacity of a composite member is evaluated based on the method of superposition. That is

$$(V_n)_{\text{comp}} = {}_sV_u + {}_rV_u \quad (1)$$

where  $(V_n)_{\text{comp}}$  = shear capacity of the concrete-encased composite member;  ${}_sV_u$  = shear capacity of steel portion; and  ${}_rV_u$  = shear capacity of reinforced concrete (RC) portion. According to the commentary on the AIJ-SRC code, the bond between the steel shape and the concrete can be neglected in the ultimate state. Thus, the shear capacity of a concrete-encased composite member is determined in such a way that the steel and RC portions resist the shear separately without bond between them.

To determine  ${}_sV_u$  and  ${}_rV_u$  in (1), it is suggested that

$${}_sV_u = \min \left( \frac{\sum {}_sM_u}{l'}, t_w \cdot d_w \cdot \frac{F_{ys}}{\sqrt{3}} \right) \quad (2)$$

$${}_rV_u = \min \left( \frac{\sum {}_rM_u}{l'}, {}_rV_{su} \right) \quad (3)$$

where  ${}_sM_u$  = flexural capacity of the steel portion;  $l'$  = clear span length of the composite member;  $t_w$  = steel web thickness;  $d_w$  = depth of the steel web;  $F_{ys}$  = yield stress of steel;  ${}_rM_u$  = flexural capacity of RC portion; and  ${}_rV_{su}$  = shear capacity in  ${}_rV_u$  controlled by shear failure of RC portion. To determine  ${}_rV_{su}$  in (3), the following formula is suggested:

$${}_rV_{su} = \min({}_rV_{su1}, {}_rV_{su2}) \quad (4)$$

where

$${}_rV_{su1} = B \cdot r \cdot j \cdot (0.5 \cdot {}_r\alpha \cdot f_s + 0.5 \cdot \rho_w \cdot F_{yh}) \quad (5)$$

$${}_rV_{su2} = B \cdot r \cdot j \cdot \left( \frac{b'}{B} \cdot f_s + \rho_w \cdot F_{yh} \right) \quad (6)$$

where  ${}_rV_{su1}$  = shear capacity in  ${}_rV_{su}$  due to diagonal shear failure of RC portion;  ${}_rV_{su2}$  = shear capacity in  ${}_rV_{su}$  due to shear bond failure of RC portion;  $B$  = gross width of composite member;  $r \cdot j$  = distance between centroids of tension and compression in RC portion under flexural;  ${}_r\alpha$  = coefficient related to shear span ratio of RC portion, conservatively taken to equal 1.0;  $f_s$  = shear stress of concrete;  $\rho_w$  = ratio of transverse reinforcement;  $F_{yh}$  = yield stress of transverse reinforcement; and  $b'$  = effective width of concrete.

### ACI BUILDING CODE (ACI 1999)

In the ACI building code, there is no clear guideline available for the shear design of concrete-encased composite members. It is also noted that no specific provision is included regarding the prevention of the shear bond failure of concrete-encased composite members. However, there are valuable provisions involving the shear design of ordinary RC structural members in the code. In the shear design of an RC member, the diagonal shear failure mode is usually the major concern of the design. In the ACI code, the shear capacity of an RC member that fails in diagonal shear can be calculated by using the following equations:

$$(V_n)_{rc} = V_r + V_c \quad (7)$$

with

$$V_r = \frac{A_v F_{yh} d}{S} \leq 0.67 \sqrt{f'_c} b d \quad (8)$$

and members subjected to shear and bending

$$V_c = 0.17 \sqrt{f'_c} b d \quad (9)$$

members subjected to shear, bending, and axial compression

$$V_c = 0.17 \left( 1 + 0.073 \frac{N_u}{A_g} \right) \sqrt{f'_c} b d \quad (10)$$

and members subjected to shear, bending, and axial tension

$$V_c = 0.17 \left( 1 + 0.29 \frac{N_u}{A_g} \right) \sqrt{f'_c} b d \quad (11)$$

where  $(V_n)_{rc}$  = shear capacity of RC member;  $V_r$  = shear contribution of the transverse reinforcement;  $V_c$  = shear contribution of the concrete portion;  $A_v$  = area of transverse reinforcement within distance  $S$ ;  $d$  = distance from extreme compression fiber to centroid of longitudinal tension reinforcements;  $S$  = spacing of transverse reinforcement;  $f'_c$  = concrete compressive strength;  $b$  = gross width of RC member;  $N_u$  = required axial compression or tension computed at factored loads; and  $A_g$  = gross area of RC member.

### AISC-LRFD SPECIFICATION (AISC 1993)

For concrete-encased composite beams, the AISC-LRFD specification states that the shear capacity should be determined by the properties of the steel section alone. The shear capacity contribution of the RC portion is conservatively neglected. For concrete-encased composite columns, the AISC-LRFD specification has no clear design guideline regarding the determination of the shear capacity of the composite columns. It is also noted that there is no related provision to avoid shear bond failure of the composite member.

### NEHRP SEISMIC PROVISIONS (BSSC 1997)

In the NEHRP provisions, the shear capacity of a composite beam follows the related provisions in the AISC-LRFD specification. However, the shear capacity of a concrete-encased composite column is taken as the sum of the contribution of the steel web plus the transverse reinforcement. The shear capacities of the steel web and the transverse reinforcement can be calculated by the formulas suggested in the AISC-LRFD specification and ACI code, respectively. It is also noted that the latest NEHRP provisions include requirements for shear connectors for encased composite columns. The existence of shear connectors between steel and concrete may help to prevent the shear bond failure of a composite column.

From the review of the shear design provisions presented in the above sections, the following observations are made: (1)

for the shear design of concrete-encased composite members, the current ACI, AISC, and NEHRP design provisions are not adequate to prevent the possible shear bond failure along the interface of the steel flange and concrete; (2) although the AII-SRC code includes detailed provisions for the shear design of concrete-encased composite members, it is noted that the format and the equations are complicated and difficult to use for engineers who are unfamiliar with Japanese building codes.

### PROPOSED APPROACH

This study presents a new approach containing the following characteristics: (1) the new approach considers both failure modes of diagonal shear failure and shear bond failure; (2) important parameters such as steel flange width, stirrup ratio, concrete strength, and applied axial load are taken into account in the proposed approach; (3) the proposed approach adheres to the conventional format of the ACI code and AISC specification so that engineers can easily use it.

### Shear Capacity of Composite Member

In the proposed approach, the shear capacity of a concrete-encased composite member can be determined as follows:

$$(V_n)_{comp} = (V_n)_s + (V_n)_{rc} \quad (12)$$

with

$$(V_n)_s = 0.6F_{ys}A_{ws} \quad (13)$$

$$(V_n)_{rc} = \min[(V_n)_{rc1}, (V_n)_{rc2}] \quad (14)$$

where  $(V_n)_s$  represents the shear capacity of steel shape in the composite member;  $(V_n)_{rc}$  denotes the shear capacity of the RC portion in the composite member;  $A_{ws}$  = area of steel web;  $(V_n)_{rc1}$  and  $(V_n)_{rc2}$  = shear capacities of the RC portion in the composite member controlled by diagonal shear failure and shear bond failure, respectively.

As indicated in (14), the shear capacity of the RC portion  $(V_n)_{rc}$  is determined as the smaller value of the diagonal shear capacity  $(V_n)_{rc1}$  and the shear bond capacity  $(V_n)_{rc2}$ . The following paragraphs will introduce how  $(V_n)_{rc1}$  and  $(V_n)_{rc2}$  are determined in the proposed approach.

### Diagonal Shear Capacity of RC Portion

It is noted that Priestley et al. (1994) investigated the diagonal shear capacity of reinforced concrete columns and pointed out the conservatism of the shear design formula suggested in the ACI code. In addition, a recommendation that the ACI shear formula needs to be revised was proposed. However, before the adoption of Priestley's recommendation by the ACI, the diagonal shear capacity  $(V_n)_{rc1}$  of a concrete-encased composite member is still calculated by using the current ACI shear design formula. That is

$$(V_n)_{rc1} = A_v F_{yh} (d/S) + 0.17 \sqrt{f'_c} B d \quad (15)$$

in which the first term should not exceed  $0.67 \sqrt{f'_c} B d$ . For a composite member subjected to shear, bending, and axial compression, the diagonal shear capacity is

$$(V_n)_{rc1} = A_v F_{yh} (d/S) + 0.17 \left( 1 + 0.073 \frac{N_u}{A_g} \right) \sqrt{f'_c} B d \quad (16)$$

### Shear Bond Capacity of RC Portion

To determine the shear bond capacity  $(V_n)_{rc2}$  of the RC portion, the shear-friction analogy is utilized in the proposed approach. As shown in Fig. 2(a), when a horizontal shear force  $V_f$  is applied to an RC specimen, the relative slip of the cracked parts causes a separation of the cracked surfaces. If there is

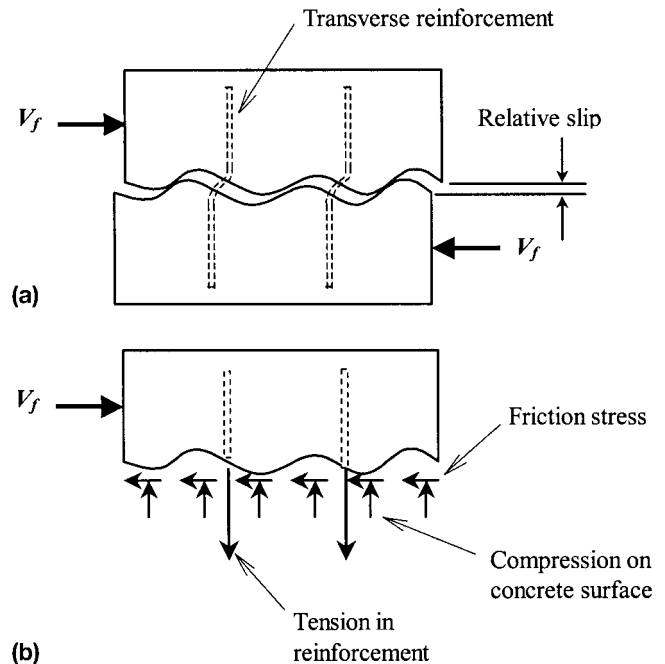


FIG. 2. Shear-Friction Analogy of RC Member (ASCE-ACI 1973): (a) Relative Slip of Cracked Parts; (b) Relation between Compression on Concrete and Tension in Reinforcement

transverse reinforcement across the crack, it is elongated by the separation of the surfaces and hence is stressed in tension. For equilibrium, compressive stresses acting on the concrete surface are needed, as shown in Fig. 2(b). It is observed that the shear force is transmitted across the cracked surface in the following ways: (1) friction resulting from the compressive stress acting on the cracked surfaces; and (2) interlock of aggregate protrusions on the cracked surfaces combined with dowel action of the reinforcement crossing the surface.

Test results on the shear friction behavior of RC members presented by Hofbeck et al. (1969) and Mattock et al. (1972) indicated that the shear friction strength of a cracked surface with transverse reinforcement perpendicular to the shear plane is given as

$$V_f = \mu_f A_v F_{yh} + K_1 A_c \leq 0.3 f'_c A_c \quad (17)$$

where  $\mu_f$  = shear friction coefficient, taken as 0.8 for concrete sliding on concrete;  $A_v$  denotes the area of transverse reinforcement crossing the shear plane;  $K_1$  represents the empirical constant, taken equal to 2.8 MPa for normal weight concrete; and  $A_c$  = area of concrete surface-resisting shear friction. The first term in (17) represents the friction force, and the second term denotes the shear transferred by shearing off surface protrusions and by dowel action.

Owing to the existence of the steel shape in a concrete-encased composite member, the shear-friction analogy of a composite member is somewhat different from that of an ordinary RC member. Thus (17) needs to be modified so that it can be useful for shear design of composite members. Fig. 3 illustrates the shear behavior in a composite member subjected to shear bond failure. Fig. 3(a) illustrates the shear bond cracks along the interfaces of steel flanges and concrete. Fig. 3(b) displays the shear-friction force along the cracked plane. From Fig. 3(b), the horizontal shear friction capacity per unit spacing  $S$  of the RC portion  $V_{hf}$  can be calculated by conservatively assuming that the contribution of the bond stress between the steel flange and concrete is negligible. That is

$$V_{hf} = \mu_f A_v F_{yh} + K_1 A_{ch} \quad (18)$$

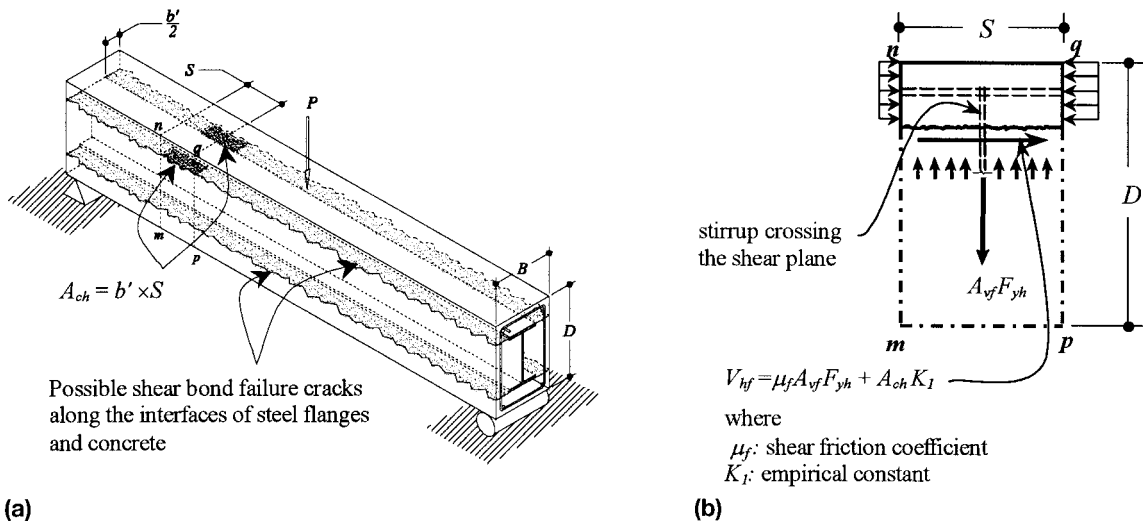


**FIG. 3.** Composite Member Subjected to Shear Bond Failure: (a) Shear Bond Failure Cracks; (b) Shear-Friction Force  $V_{hf}$  along Cracked Plane

where  $A_{ch}$  = area of concrete resisting the horizontal shear friction force within a distance  $S$ , taken as  $S \times b'$ ;  $S$  = spacing of transverse reinforcement;  $b'$  = effective width of the concrete section to resist shear bond failure, taken as  $(B - b_f)$ ;  $B$  and  $b_f$  are the widths of the gross section and the steel flange, respectively.

From (18), the maximum average shear stress provided by internal shear friction force on the cracked surface within a distance  $S$ ,  $\tau_1$  can be expressed as

$$\tau_1 = \frac{V_{hf}}{b'S} \quad (19)$$

The use of  $b'$  in (19) is to show the fact that if the steel flange width becomes larger and approaches the overall width of the composite section, the horizontal shear resistance provided by the concrete portion along the interface of the steel flange and concrete will approach zero.

The shear stress resulting from applied shear force  $V_{rc}$  of the RC portion at the location of the cracked surface  $\tau_2$  can be computed from

$$\tau_2 = \frac{V_{rc} Q}{I_c b'} \quad (20)$$

where  $Q$  denotes the first moment of the concrete area above the interface about the neutral axis of the RC portion; and  $I_c$  = moment of inertia of the RC portion. It is noted that (20) applies to uncracked elastic concrete members and is only an approximation for cracked concrete members (MacGregor 1997). To simplify the calculation, the average shear stress is assumed as uniformly distributed on the effective concrete area of  $A_{cv}$ , in which  $A_{cv}$  is taken as  $b' \times d$ . Thus

$$\tau_2 = \frac{V_{rc}}{b'd} \quad (21)$$

To prevent the shear bond failure, the shear stress resulting from applied shear force  $\tau_2$  should not be larger than the shear stress provided by internal shear friction force  $\tau_1$ . That is

$$\frac{V_{rc}}{b'd} \leq \frac{V_{hf}}{b'S} \quad (22)$$

Substituting (18) into (22) and with  $b'$  replaced by  $(B - b_f)$  leads to

$$V_{rc} \leq \mu_f A_v F_{yh} (d/S) + K_1 (B - b_f) d \quad (23)$$

Eq. (23) implies that the shear bond capacity of the RC portion,  $(V_n)_{rc2}$ , can be expressed as

$$(V_n)_{rc2} = \mu_f A_v F_{yh} (d/S) + K_1 (B - b_f) d \quad (24)$$

It is important to observe that  $(V_n)_{rc2}$  decreases linearly with an increase of the steel flange width. The linear correlation exists because the following simplifications are made: (1) the shear stress  $\tau_2$  along the interface of the steel flange and concrete is calculated by using the average shear stress on the effective concrete area of  $A_{cv}$ ; and (2) the contribution of the bond stress between the steel shape and the concrete is conservatively neglected.

Consequently, the shear capacity of the RC portion of the concrete-encased composite member should be the smaller value of (16) and (24).

## VERIFICATION ANALYSIS

To investigate the accuracy and suitability of the proposed approach, a verification analysis between the test results and the predictions of the proposed approach and the AIJ-SRC code (AIJ 1987) is made in this study. The test results listed in Table 1 were conducted by Zhang et al. (1993). All specimens had a square section of  $125 \times 125$  mm and were rein-

**TABLE 1.** Dimensions, Material Properties, and Test Results of Composite Members Done by Zhang et al. (1992)

Specimen number	$B \times D$ (mm)	Steel section ( $d_s \times b_f \times t_w \times t_f$ ) (mm)	Stirrups ratio [ $\rho_w = A_w / (B \times S)$ ] (%)	$F_{ys}$ (MPa)	$F_{yh}$ (MPa)	$f'_c$ (MPa)	$N_u$ (kN)	$V_{test}$ (kN)
1	125 × 125	H-80 × 80 × 2.0 × 2.0	0.23	254	297	43.9	294	52.7
2	125 × 125	H-80 × 60 × 2.0 × 2.0	0.23	270	297	32.6	121	57.1
3	125 × 125	H-80 × 60 × 2.0 × 2.0	0.23	270	297	28.0	217	57.1
4	125 × 125	H-80 × 60 × 2.0 × 2.0	0.23	270	297	31.6	483	55.9
5	125 × 125	H-50 × 60 × 3.2 × 3.2	0.23	290	297	32.8	223	54.9

Note: All specimens had concrete cover of 15 mm and reinforced by deformed bars 10 mm in diameter deployed at four corners; smooth round bars 3 mm in diameter were used as shear reinforcement every 50 mm along shear span;  $N_u$  = applied axial force;  $V_{test}$  = tested shear strengths of specimens.

forced by deformed bars 10 mm in diameter at four corners. Smooth round bars 3 mm in diameter were used as stirrups every 50 mm along the shear span. The encased wide flange steel was built up by fillet welding from a steel plate 2 or 3.2 mm in thickness. The test setup is shown in Fig. 4(a). A typical crack pattern and failure mode of the selected specimens at the ultimate state are illustrated in Fig. 4(b). From Fig. 4(b), it is observed that all specimens listed in Table 1 failed in the shear bond failure condition.

Table 2 shows the comparative results between the test results and the predicted shear strengths based on the proposed approach and the AIJ-SRC code (AIJ 1987). The predictions of the ACI, AISC, and NEHRP design provisions are not listed in this table; owing to these provisions does not provide formulas to calculate the shear strength controlled by the shear bond failure.

From Table 2, it is observed that the average ratios of the predicted value to the test result are 0.938 with a standard deviation of 0.05 for the proposed approach, and 0.921 with a standard deviation of 0.037 for the AIJ-SRC code. Considering the above observation, it is felt that the shear capacity of a composite member can be satisfactorily predicted by the proposed approach.

In addition, Table 2 indicates that the shear strengths predicted by the proposed approach are controlled by the shear bond failure mode for all specimens. However, only the shear

strength of Specimen No. 1 predicted by the AIJ-SRC code is controlled by the shear bond failure mode. This observation shows that the proposed approach can more reasonably predict the shear failure mode of a composite member than the AIJ-SRC code. This is mainly because the formulas for predicting shear strength of a composite member given in the AIJ-SRC code [(5) and (6)] does not involve the axial force effect on the shear capacity of the concrete portion.

Although the tested specimens listed in Table 1 were small in scale, the writers consider that the experiments conducted by Zhang and Yamada (1993) are still valuable in illustrating the shear failure mechanism of composite members due to the lack of published research reported on large-scale test specimens. To further investigate the influence of the scale factor, it is suggested that large-scale tests on the shear behavior of composite members will be needed for future studies.

### PARAMETRIC STUDY

Figs. 5–7 summarize the influence of the major parameters, including the steel flange width, stirrup ratio, concrete compressive strength, and applied axial load on the shear strengths of concrete-encased composite members. In these figures, the horizontal axis denotes the ratio of the steel flange width to the gross width of the composite section  $b_f/B$ , and the vertical axis represents the shear capacity of the composite member

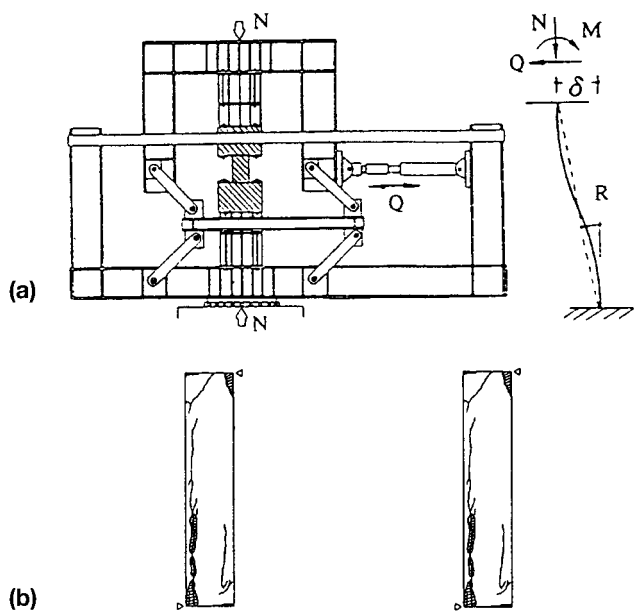


FIG. 4. Physical Test Conducted by Zhang et al. (1993): (a) Test Setup and Loading System; (b) Typical Crack Pattern and Failure Mode of Specimens

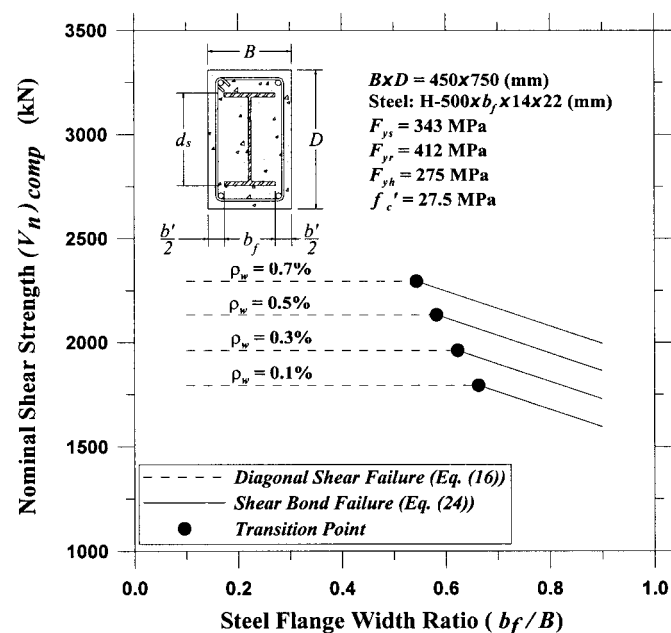


FIG. 5. Influence of Steel Flange Width  $b_f$  and Stirrup Ratio  $\rho_w$  on Shear Strength

TABLE 2. Comparisons of Shear Strengths Predicted by AIJ-SRC Code and Proposed Method with Test Results Done by Zhang et al. (1992)

Specimen number	$V_{test}$		$(V_n)_{AIJ}^a$		$(V_n)_{prop}^b$		$\frac{(V_n)_{AIJ}}{V_{test}}$	$\frac{(V_n)_{prop}}{V_{test}}$
	(kN)	Failure mode	(kN)	Failure mode	(kN)	Failure mode		
1	52.7	SB <sup>c</sup>	49.8	SB <sup>c</sup>	45.6	SB <sup>c</sup>	0.945	0.865
2	57.1	SB <sup>c</sup>	51.3	DS <sup>d</sup>	53.3	SB <sup>c</sup>	0.898	0.933
3	57.1	SB <sup>c</sup>	50.1	DS <sup>d</sup>	53.3	SB <sup>c</sup>	0.877	0.933
4	55.9	SB <sup>c</sup>	51.1	DS <sup>d</sup>	53.3	SB <sup>c</sup>	0.914	0.953
5	54.9	SB <sup>c</sup>	53.2	DS <sup>d</sup>	55.2	SB <sup>c</sup>	0.969	1.005
							Average: 0.921	0.938
							Standard deviation: 0.037	0.050
							Coefficient of variation: 0.040	0.054

<sup>a</sup> $(V_n)_{AIJ}$  = shear strength predicted by AIJ-SRC code (AIJ 1987).

<sup>b</sup> $(V_n)_{prop}$  = shear strength predicted by proposed approach.

<sup>c</sup>SB = shear bond failure.

<sup>d</sup>DS = diagonal shear failure.

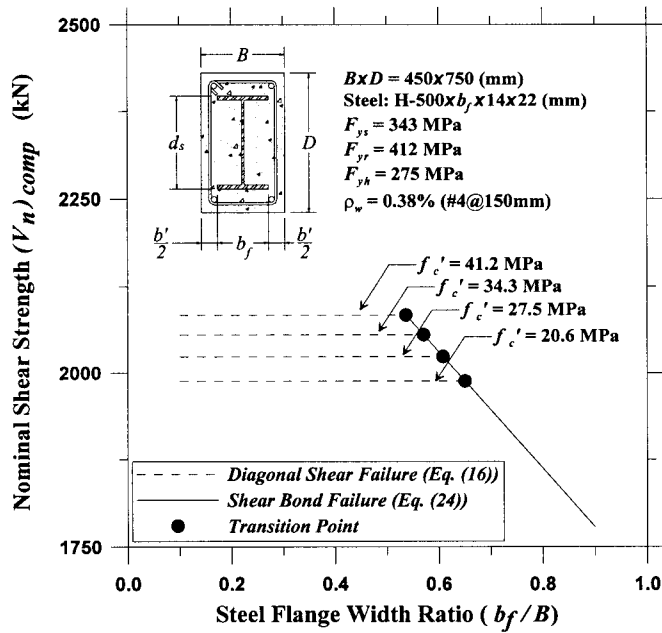


FIG. 6. Influence of Steel Flange Width  $b_f$  and Concrete Compressive Strength  $f'_c$  on Shear Strength

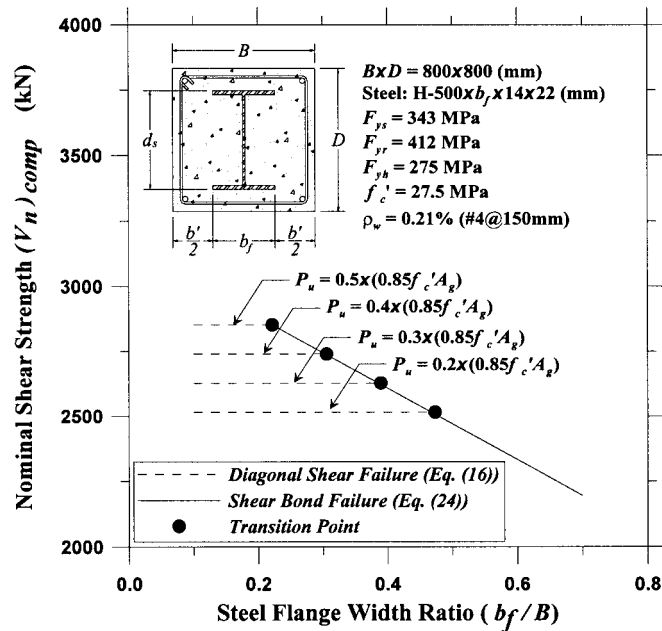


FIG. 7. Influence of Steel Flange Width  $b_f$  and Applied Axial Load  $P_u$  on Shear Strength

$(V_n)_{comp}$ . From these figures, it is observed that the proposed approach contains the following characteristics:

1. For every curve shown in these figures, a transition point (shown as a large solid circle) exists between the two envelopes of the diagonal shear failure mode and the shear bond failure mode. The steel flange width ratio at the transition point is given the name "critical steel flange ratio  $(b_f/B)_{cr}$ ." It is observed that the shear capacity of the composite member is controlled by the diagonal shear failure mode when the value of  $(b_f/B)$  is smaller than the critical ratio  $(b_f/B)_{cr}$ . On the contrary, the shear capacity is governed by the shear bond failure mode when  $(b_f/B)$  exceeds  $(b_f/B)_{cr}$ .
2. As observed from Figs. 5–7, all the envelopes representing the diagonal shear failure mode appear as broken

horizontal lines. This observation implies that the steel flange width ratio does not affect the shear capacity under the diagonal shear failure mode. However, if the shear bond failure mode controls the shear design, the shear capacity drastically decreases as the steel flange width ratio increases.

3. Fig. 5 reveals that the increase of the stirrup ratio gives rise of both the shear capacities of the diagonal shear and the shear bond failure modes. Figs. 6 and 7 indicate that the increase of concrete compressive strength or the applied axial load results in an increase of resistance to the diagonal shear failure.

### CRITICAL STEEL FLANGE RATIO

The critical steel flange ratio  $(b_f/B)_{cr}$  is useful in distinguishing between the diagonal shear failure mode and shear bond failure mode. This ratio can be derived from (16) and (24). Let these two equations be equal, which yields

$$\left(\frac{b_f}{B}\right)_{cr} = 1 - \frac{1}{K_1} \left[ 0.17 \left( 1 + 0.073 \frac{N_u}{A_g} \right) \sqrt{f'_c} + (1 - \mu_f) \rho_w F_{yh} \right] \quad (25)$$

The proposed formula [(25)], reveals the following characteristics of the critical ratio: (1) the critical ratio is a linear function of the stirrup ratio  $\rho_w$  and applied axial load  $N_u$ . Also, the critical ratio decreases with increasing of the stirrup ratio or applied axial load; and (2) the critical ratio decreases linearly with a radical expression of concrete compression strength  $f'_c$ .

From the above observations, it is important to note that the critical steel flange ratio  $(b_f/B)_{cr}$  of a composite member may become smaller if the stirrup ratio, concrete compressive strength, or applied axial load are increased. It is likely that the shear bond failure mode may control the shear design of a composite member if the critical steel flange ratio becomes smaller.

### COMPARISONS OF RESULTS PREDICTED BY PROPOSED APPROACH AND EXISTING CODES

This study compares the shear capacities predicted by using the proposed approach, the AIJ-SRC code (AIJ 1987), the ACI code (ACI 1999), the AISC-LRFD specification (AISC 1993), and the NEHRP provisions (BSSC 1997). Table 3 lists the dimensions and material properties of the assumed composite members used in this study, where specimens are arranged with varying steel flange widths and stirrup ratios, respectively. Tables 4 and 5 summarize the calculated shear capacities reflecting the influences of the steel flange width and the stirrup

TABLE 3. Dimensions and Material Properties of Assumed Composite Members

Specimen number	$B \times D$ (mm)	$b_f$ (mm)	$\rho_w$ (%)	$f'_c$ (MPa)
1	450 × 750	225	0.38	27.5
2	450 × 750	250	0.38	27.5
3	450 × 750	275	0.38	27.5
4	450 × 750	300	0.38	27.5
5	450 × 750	325	0.38	27.5
6	450 × 750	275	0.2	27.5
7	450 × 750	275	0.3	27.5
8	450 × 750	275	0.4	27.5
9	450 × 750	275	0.5	27.5
10	450 × 750	275	0.6	27.5

Note: Steel section: H-500 ×  $b_f$  × 14 × 22 (mm); designation of steel section: H- $d_s$  ×  $b_f$  ×  $t_w$  ×  $t_f$ ;  $F_{y_s}$  = 343 MPa;  $F_{y_r}$  = 412 MPa;  $F_{y_h}$  = 275 MPa; concrete cover from steel flange surface is 125 mm; concrete cover from center of rebar is 70 mm.

**TABLE 4.** Influence of Steel Flange Width on Shear Capacity of Composite Members

Specimen number	Design method	$(V_n)_s^a$ (kN)	$(V_n)_{rc}^b$ (kN)		$(V_n)_{comp}^c$ (kN)	Controlled failure mode
			Diagonal shear	Shear bond		
1	Proposed	1,442	582	673	2,024	DS <sup>d</sup>
1	AIJ-SRC	1,388	599	737	1,987	DS <sup>d</sup>
1	ACI <sup>e</sup>	1,442	582	—	2,024	DS <sup>d</sup>
1	AISC and NEHRP	1,442	—	—	1,442	NA <sup>f</sup>
2	Proposed	1,442	582	626	2,024	DS <sup>d</sup>
2	AIJ-SRC	1,388	599	686	1,987	DS <sup>d</sup>
2	ACI <sup>e</sup>	1,442	582	—	2,024	DS <sup>d</sup>
2	AISC and NEHRP	1,442	—	—	1,442	NA <sup>f</sup>
3	Proposed	1,442	582	579	2,021	SB <sup>g</sup>
3	AIJ-SRC	1,388	599	635	1,987	DS <sup>d</sup>
3	ACI <sup>e</sup>	1,442	582	—	2,024	DS <sup>d</sup>
3	AISC and NEHRP	1,442	—	—	1,442	NA <sup>f</sup>
4	Proposed	1,442	582	533	1,975	SB <sup>g</sup>
4	AIJ-SRC	1,388	599	583	1,971	SB <sup>g</sup>
4	ACI <sup>e</sup>	1,442	582	—	2,024	DS <sup>d</sup>
4	AISC and NEHRP	1,442	—	—	1,442	NA <sup>f</sup>
5	Proposed	1,442	582	486	1,928	SB <sup>g</sup>
5	AIJ-SRC	1,388	599	532	1,920	SB <sup>g</sup>
5	ACI <sup>e</sup>	1,442	582	—	2,024	DS <sup>d</sup>
5	AISC and NEHRP	1,442	—	—	1,442	NA <sup>f</sup>

<sup>a</sup> $(V_n)_s$  = nominal shear strength of steel part, taken as  $0.6F_{ys}A_{ws}$ , except  $0.577F_{ys}A_{ws}$  for AIJ-SRC code.

<sup>b</sup> $(V_n)_{rc}$  = nominal shear strength of RC part, taken as smaller of diagonal shear and shear bond capacity.

<sup>c</sup> $(V_n)_{comp}$  = nominal shear strength of composite member =  $(V_n)_s + (V_n)_{rc}$ .

<sup>d</sup>DS = diagonal shear failure.

<sup>e</sup>Values include shear capacity of steel web.

<sup>f</sup>NA = not applicable.

<sup>g</sup>SB = shear bond failure.

**TABLE 5.** Influence of Stirrup Ratio on Shear Capacity of Composite Members

Specimen number	Design method	$(V_n)_s^a$ (kN)	$(V_n)_{rc}^b$ (kN)		$(V_n)_{comp}^c$ (kN)	Controlled failure mode
			Diagonal shear	Shear bond		
6	Proposed	1,442	433	460	1,875	DS <sup>d</sup>
6	AIJ-SRC	1,388	534	504	1,892	SB <sup>e</sup>
6	ACI <sup>f</sup>	1,442	433	—	1,875	DS <sup>d</sup>
6	AISC and NEHRP	1,442	—	—	1,442	NA <sup>g</sup>
7	Proposed	1,442	520	530	1,962	DS <sup>d</sup>
7	AIJ-SRC	1,388	572	580	1,960	DS <sup>d</sup>
7	ACI <sup>f</sup>	1,442	520	—	1,962	DS <sup>d</sup>
7	AISC and NEHRP	1,442	—	—	1,442	NA <sup>g</sup>
8	Proposed	1,442	605	598	2,047	SB <sup>e</sup>
8	AIJ-SRC	1,388	609	655	1,997	DS <sup>d</sup>
8	ACI <sup>f</sup>	1,442	605	—	2,047	DS <sup>d</sup>
8	AISC and NEHRP	1,442	—	—	1,442	NA <sup>g</sup>
9	Proposed	1,442	690	666	2,108	SB <sup>e</sup>
9	AIJ-SRC	1,388	647	730	2,034	DS <sup>d</sup>
9	ACI <sup>f</sup>	1,442	690	—	2,132	SB <sup>e</sup>
9	AISC and NEHRP	1,442	—	—	1,442	NA <sup>g</sup>
10	Proposed	1,442	772	731	2,173	SB <sup>e</sup>
10	AIJ-SRC	1,388	682	801	2,070	DS <sup>d</sup>
10	ACI <sup>f</sup>	1,442	772	—	2,214	DS <sup>d</sup>
10	AISC and NEHRP	1,442	—	—	1,442	NA <sup>g</sup>

<sup>a</sup> $(V_n)_s$  = nominal shear strength of steel part, taken as  $0.6F_{ys}A_{ws}$ , except  $0.577F_{ys}A_{ws}$  for AIJ-SRC code.

<sup>b</sup> $(V_n)_{rc}$  = nominal shear strength of RC part, taken as smaller of diagonal shear and shear bond capacity.

<sup>c</sup> $(V_n)_{comp}$  = nominal shear strength of composite member =  $(V_n)_s + (V_n)_{rc}$ .

<sup>d</sup>DS = diagonal shear failure.

<sup>e</sup>SB = shear bond failure.

<sup>f</sup>Values include shear capacity of steel web.

<sup>g</sup>NA = not applicable.

ratio, respectively. From these tables, the following observations are made:

1. The shear capacities predicted by using the proposed approach and the AIJ-SRC code are found to be quite close. This closeness is attributed primarily to that these two approaches consider both of the shear bond failure mode as well as the diagonal shear failure mode.
2. The values predicted by using the AISC-LRFD specification are the most conservative among the five approaches. This is mainly because the shear capacity contribution of the RC portion is conservatively neglected in the AISC-LRFD specification.
3. It is interesting to observe from Table 4 that the shear capacities predicted by using the ACI code are constant for all specimens. For example, the variations of the steel flange width from 225 to 325 mm (Specimens 1–5, shown in Table 3) have no influence on the shear resistance of the concrete portion. This observation indicates that the current ACI approach does not consider the effect of the variation of steel flange width on the shear capacity of a concrete-encased composite member. It is obvious that if the steel flange width becomes larger and approaches the overall width of the composite section, the possibility for this section to fail along the interface of the steel flange and concrete will become much higher.
4. In the current ACI, AISC, and NEHRP design provisions, the influences of the steel flange width, shear reinforcement, concrete compressive strength, and applied axial load on the shear capacity of composite members have not been adequately addressed. In this study, the pro-

posed approach takes all these important parameters into account and shows their influences on the shear capacities of concrete-encased composite members (Figs. 5–7).

## SUMMARY AND CONCLUSIONS

This research attempted to clarify the influence of shear bond failure on the shear strength of concrete-encased composite structural members. Important parameters such as the steel flange width, stirrup ratio, concrete strength, and applied axial load were considered in the development of a new method for the shear strength prediction. Each of the parameters was studied in-depth to show its effect on the shear strength of a composite member.

In addition, this study introduced a new term called “the critical steel flange ratio  $(b_f/B)_{cr}$ ” to distinguish the diagonal shear failure mode from the shear bond failure mode. It was found that when the steel flange ratio  $(b_f/B)$  of a composite section is larger than the critical steel flange ratio  $(b_f/B)_{cr}$ , the shear capacity will be governed by the shear bond failure mode. On the contrary, the diagonal shear failure mode controls the shear capacity if the ratio of  $(b_f/B)$  is smaller than  $(b_f/B)_{cr}$ .

To evaluate the accuracy of the proposed approach, a verification analysis between test results done by other researchers and the predictions of the proposed approach was made in this study. The results showed that the proposed approach can satisfactorily predict the shear capacity of a composite member.

The shear capacities predicted by the proposed approach were also compared with the values calculated by using ex-

isting American and Japanese codes. It was noted that in the current U.S. design practice, there is no specific design provision available regarding the shear bond failure of a fully encased composite structural member. It was the major objective of the proposed approach to take into account the influence of the shear bond failure along the interface of the concrete and steel flange on the shear capacity of a composite member.

For future study, tests of large-scale specimens need to be conducted to investigate the shear failure mechanism of concrete-encased composite structural members.

## ACKNOWLEDGMENT

The financial support of the National Science Council of Taiwan, R.O.C., is gratefully acknowledged.

## REFERENCES

- Architectural Institute of Japan (AIJ). (1987). *Standards for structural calculation of steel reinforced concrete structures*, Tokyo.
- American Concrete Institute (ACI). (1999). "Buildings code requirements for structural concrete." *ACI 318-99*, Detroit.
- ASCE-ACI Task Committee 426. (1973). "The shear strength of reinforced concrete members." *J. Struct. Div.*, ASCE, 99(6), 1091-1187.
- American Institute of Steel Construction (AISC). (1993). *Load and resistance factor design specification for structural steel buildings*, 2nd Ed., Chicago.
- Building Seismic Safety Council (BSSC). (1997). *NEHRP recommended provisions for the development of seismic regulations for new buildings and other structures*, Washington, D.C.
- Goel, S. C. (1997). "U.S.-Japan cooperative earthquake research program: Phase 5—Composite and hybrid structures." *Proc., Summary, Resolutions and Recommendations of the 4th Joint Tech. Coordinating Meeting*, Dept. of Civ. Engrg., University of Michigan, Ann Arbor, Mich.
- Hofbeck, J. A., Ibrahim, I. O., and Mattock, A. H. (1969). "Shear transfer in reinforced concrete." *ACI J.*, 66(2), 119-128.
- MacGregor, J. G. (1997). *Reinforced concrete: Mechanics and design*, 3rd Ed., Prentice-Hall, Englewood Cliffs, N.J.
- Mattock, A. H., and Hawkins, N. M. (1972). "Shear transfer in reinforced concrete—Recent research." *J. Prestressed Concrete Inst.*, 17(2), 55-75.
- Nishiyama, I., Goel, S. C., and Yamanouchi, H. (1998). "U.S.-Japan cooperative earthquake research program: Phase 5—Composite and hybrid structures." *Proc., Summary, Resolutions and Recommendations of the 5th Joint Tech. Coordinating Meeting*, Dept. of Civ. Engrg., University of Michigan, Ann Arbor, Mich.
- Priestley, M. J. N., Seible, F., Xiao, Y., and Verma, R. (1994a). "Steel jacket retrofitting of reinforced concrete bridge columns for enhancing shear strength—Part 1: Theoretical considerations and test design." *ACI Struct. J.*, 91(4), 394-405.
- Priestley, M. J. N., Seible, F., Xiao, Y., and Verma, R. (1994b). "Steel jacket retrofitting of reinforced concrete bridge columns for enhancing shear strength—Part 2: Test results and comparison with theory." *ACI Mat. J.*, 91(5), 537-551.
- Ricles, J. M., and Paboojian, S. D. (1994). "Seismic performance of steel-encased composite columns." *J. Struct. Engrg.*, ASCE, 120(8), 2474-2494.
- Wakabayashi, M. (1988). "A historical study of research on composite construction in Japan." *Proc., Compos. Constr. in Steel and Concrete Conf.*, ASCE, New York, 400-427.
- Zhang, F., and Yamada, M. (1993). "Composite columns subjected to bending and shear." *Proc., Compos. Constr. in Steel and Concrete II*, ASCE, New York, 483-498.